Heliyon 10 (2024) e29556

Contents lists available at ScienceDirect

Heliyon

journal homepage: www.cell.com/heliyon

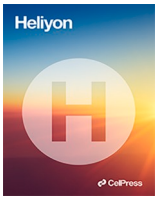

Research article

Huanglian Jiedu decoction alleviates neurobehavioral damage in mice with chronic alcohol exposure through the RAS-RAF-MEK-ERK pathway

Yun Chen [a,b], Lianyan Jiang [a], Mao Li [c], Yuling Shen [a], Shanyu Liu [a], Dongdong Yang [d,*]

[a] Department of Neurology, Chengdu University of Traditional Chinese Medicine, Sichuan, PR China
[b] Department of Neurology, The First People's Hospital of Bijie City, Guizhou, PR China
[c] Department of Neurology, The First Affiliated Hospital of Henan University of Traditional Chinese Medicine, Zhengzhou, PR China
[d] Department of Neurology, The Affiliated Hospital of Chengdu University of Traditional Chinese Medicine, Sichuan, PR China

ARTICLE INFO

Keywords:
Huanglian jiedu decoction
Chronic alcohol exposure
Behavioral change
Transcriptome sequencing
RAS-RAF-MEK-ERK pathway

ABSTRACT

Objective: Long-term alcohol consumption can cause organic damage to the brain, resulting in mental and nervous system abnormalities and intellectual impairment. Huanglian Jiedu decoction (HLJDD) is the classic representative of clearing heat and detoxifying. This study aimed to explore the effects and possible mechanisms of HLJDD on brain injury in chronic alcohol-exposed mice.

Methods: The alcohol-exposed mice were treated with different doses of HLJDD to observe behavioral changes, hippocampal $A\beta_{1\text{-}42}$ deposition, number and ultrastructural changes of neurons in the hippocampus and prefrontal cortex, and expressions of synaptic proteins. On this basis, transcriptome sequencing was used to analyze the differentially expressed genes in different treatment groups, and functional enrichment analysis was performed. Then, WB and RT-PCR were used to verify the expression of the pathway.

Results: Chronic alcohol exposure reduced body weight in mice, led to motor cognitive impairment, increased $A\beta_{1\text{-}42}$ in the hippocampus, decreased the number of neurons in the hippocampus and prefrontal cortex, and the expression of PSD95 and SYN in the hippocampus. HLJDD significantly improved the cognitive dysfunction of mice and alleviated the damage of the hippocampus and prefrontal cortex. Transcriptome sequencing results showed that the regulatory effects of HLJDD on chronic alcohol-exposed mice may be related to the RAS pathway. Further experiments confirmed that chronic alcohol exposure caused a significant increase in protein and gene expressions of the RAS-RAF-MEK-ERK pathway in mouse, and this activation was reversed by HLJDD.

Conclusion: HLJDD may ameliorate brain damage caused by chronic alcohol exposure by regulating the RAS-RAF-MEK-ERK pathway.

* Corresponding author. Department of Neurology, The Affiliated Hospital of Chengdu University of Traditional Chinese Medicine, Sichuan 610000, PR China.
E-mail address: dongdongyang2020@163.com (D. Yang).

https://doi.org/10.1016/j.heliyon.2024.e29556
Received 3 December 2023; Received in revised form 9 April 2024; Accepted 10 April 2024
Available online 12 April 2024

1. Introduction

Alcohol abuse has become a global medical and social problem. Short-term moderate drinking does not pose an obvious threat to physical health, but long-term chronic drinking can cause organ and tissue poisoning, the most serious of which is damage to brain tissue, which can lead to memory loss, consciousness disorders, and other related symptoms, and induce addiction [1,2]. Long-term and continuous drinking directly affects the absorption of vitamins and other nutrients, resulting in nutritional deficiency, especially vitamin B (VB) deficiency leads to reduced thiamine phosphate, glucose metabolism disorders, lack of energy supply to nervous tissue, affects the synthesis and metabolism of nerve myelin substances phospholipids, and causes central and peripheral nerve demyelination and axonal degeneration [3,4]. The incidence of alcohol toxicity diseases caused by long-term drinking showed an increasing trend year by year [5]. Studies have shown that long-term drinking can make the incidence of neurological disorders, cardiovascular and cerebrovascular diseases higher than the general population [6]. It is generally believed that alcoholic encephalopathy including Wernicke's encephalopathy, alcoholic delusional disorder, Korsakov's psychosis, alcoholic hypoglycemic encephalopathy, alcoholic dementia, emotional disorder caused by alcoholism, personality change caused by alcoholism, etc., can seriously threaten people's life, health and quality of life [7]. It is of great practical significance to investigate the pathogenesis and possible treatment of alcoholic encephalopathy.

Huanglian Jiedu decoction (HLJDD) is a classic Chinese medicine compound, that originated from Ge Hong's "Handbook of Prescriptions for Emergencies". It is composed of sovereign medicinal *Coptis chinensis* Franch., minister medicinal *Scutellaria baicalensis* Georgi, assistant medicinal *Phellodendron chinense* Schneid. and courier medicinal *Gardenia jasminoides J.* Ellis, which can achieve the effect of clearing heat, purging fire, and detoxifying. Modern pharmacological studies have found that it has anti-inflammatory, antioxidant, anti-cerebral ischemia, neuronal protection, and other effects, and can be used in the treatment of cerebrovascular diseases, dementia, and other diseases [8–10]. Studies have shown that HLJDD can inhibit the progression of Alzheimer's disease (AD) by remodeling the peripheral microenvironment through the "brain-gut" axis [11], and also has a strong antithrombotic effect in the rat model of cerebral apoplexy induced by ischemia reperfusion [12]. However, the protective effect and the underlying mechanism of HLJDD on chronic alcohol exposure brain injury are unclear.

Therefore, in this study, chronic alcohol exposure was used to build a mouse model, and behavioral changes as well as damage to the hippocampus and prefrontal cortex of mice were analyzed after low, medium, and high doses of HLJDD treatment. Moreover, differential expression genes and differential signaling pathways were explored based on transcriptome sequencing, and their possible mechanisms were analyzed.

2. Material and methods

2.1. Preparation of HLJDD

HLJDD was prepared by routine decoction with water (1:10, w/v) according to the original formula compatibility ratio of 3:2:2:3 (i.e. *Coptis chinensis* Franch. 9 g, *Scutellaria baicalensis* Georgi 6 g, *Phellodendron chinense* Schneid. 6 g, *Gardenia jasminoides J.* Ellis 9 g). After concentration, the decoction was adjusted to the concentration of 2 g/ml, and stored in the refrigerator at 4 °C.

2.2. Analysis of the main components of HLJDD

The components of HLJDD were qualitatively analyzed by LC-MS/MS method. The HLJDD extract (100 mg) was dissolved in 1 mL methanol (HPLC grade), extracted by shock, filtered by 0.22 μm membrane filter, centrifuged at 12000 rpm for 10 min, and supernatant was obtained. The liquid chromatography equipment was Ultimate 3000 (Thermo Fisher, USA), and Sepax GP-C18 Column (1.8 μm, 2.1 mm × 150 mm) was used for analysis, and the column temperature was 40 °C. The mobile phases were A (0.1 % formic acid aqueous solution, v/v) and B (100 % acetonitrile), the flow rate was 0.3 mL/min, and the gradient elution time was 5 % B at 0–10 min; 70 % B at 10–17 min; 100 % B at 17–18 min; 5 % B at 19–21 min. The mass spectrometry experiments were performed using a mass spectrometer (TripleTOF5600+, AB SCIEX, USA) in electrospray ionization (ESI) positive and negative ion modes. The ESI source conditions are as follows: Gas 1: 50, Gas 2: 50, Curtain Gas: 25, Source Tempreture: 500 °C (positive ion) and 450 °C (negative ion), Ion Sapary Voltage Floating 5500 V (positive ion) and 4400 V (negative ion), TOF MS scan range: 100–1200 Da, product ion scan range: 50–1000 Da, TOF MS scan accumulation time 0.2 s, product ion scan accumulation time 0.01 s, secondary mass spectrometry was obtained using information-dependent acquisition (IDA) and high sensitivity mode, Declustering potential (DP): ±60 V, Collision Energy: 35 ± 15 eV. The files acquired by mass spectrometry were preprocessed by MS-DIAL 4.70 software. The fingerprint of each component of HLJDD was searched regarding MassBank, Respect, and GNPS databases.

2.3. Animals experimental design

A total of 36 SPF C57BL/6J male mice, 7 weeks old, about 20 g, were purchased from Chengdu DOSSY Experimental Animal Co., LTD., the license number is SCXK (chuan) 2022-039. The mice were raised in a standard SPF environment with a 12-h day and night cycle, and all operations were approved by the Experimental Animal Ethics Committee of Chengdu University of Traditional Chinese Medicine (No. 2022-59). The experiment was divided into control group, model group, model + low-dose of HLJDD group (L-HLJDD), model + medium-dose of HLJDD group (M-HLJDD), model + high-dose of HLJDD group (H-HLJDD) and model + VB1 group (positive drug). Mice in the model group were treated with the modified "drinking in the dark" (DID) procedures [13,14], that is, after entering

the first hour of the dark cycle, the water bottles of all mice were removed, and the control group was given a sweet solution of 0.066 % (w/v) saccharin, while the model group was given a sweet solution of 20 % (v/v) alcohol and 0.066 % (w/v) saccharin for 4 h. The mice were given water at other times. After 8 days of alcohol treatment, L-HLJDD, M-HLJDD, and H-HLJDD groups were given 2.28, 4.55, and 9.1 g/kg HLJDD by intragastric administration, respectively [15], the VB1 group was given 1.7 mg/kg VB1, and the control and model group were given the same amount of normal saline for 20 days. Each group was treated with or without alcohol continuously for a total of 28 days. On the last day, mice in each group were tested by open field and Morris water maze test. After the experiment, the mice were sacrificed for cervical dislocation after deep anesthesia, and the brain tissue was collected for follow-up detection.

2.4. Behavioral detection

The behavioral and cognitive abilities of mice were evaluated by open field and water maze experiments. The mice were transported to the behavioral laboratory in advance and adapted to the environment for 12 h to reduce animal stress. For the open field experiment, mice were placed in the center of a box-shaped open field device (50 cm × 50 cm × 50 cm), and the video recording system was turned on to record the activities of mice in the open field for 5 min. For the water maze experiment, during the training phase, the mice were placed in the water with their heads facing the wall of the pool, and the time (seconds) between the time the animals were placed in the water and the time they found the underwater platform was recorded. If more than 90 s, guide the animal to the platform. After 5 days of continuous training, the exploration experiment was carried out, the platform was removed, and the mice were placed into the water at the same entry points. The swimming path of the mice was recorded, and the spatial positioning ability of the mice was observed, as well as the changes in the process of space exploration.

2.5. Hematoxylin-eosin staining

Hippocampus and prefrontal cortex tissues were fixed with 4 % paraformaldehyde, and then sectioned after paraffin embedding. After routine dewaxing of the tissue sections to water, histopathological hematoxylin-eosin staining (HE) was performed. After staining, gradient alcohol was dehydrated, xylene was transparent, and neutral gum was sealed and observed under microscope (BA400Digital, Panthera, China).

2.6. Immunohistochemical staining

The paraffin sections were dewaxed to water, and antigen repair was performed with citrate buffer (PH 6.0, ZLI-9065, ZSBIO, China). Endogenous peroxidase was blocked by 3 % hydrogen peroxide, and goat serum (AR1009, Bosterbio) was used to block at room temperature for 20 min. The primary antibody $A\beta_{1\text{-}42}$ (1:200, ab201060, Abcam, UK) was incubated at 4 °C overnight, and the secondary antibody HRP- labeled goat anti-rabbit IgG (1:100, GB23303, Servicebio, China) was added and incubated at 37 °C for 30 min for immune reaction. Fresh DAB color development solution was developed at room temperature, and the slices were washed with distilled water to terminate color development. Hematoxylin re-stained the nuclei for 3 min and washed with water. The sections were sealed after dehydration and observed under the microscope (BA400Digital, Panthera, China).

2.7. Nissl staining

The tissues of the hippocampus and prefrontal cortex were dehydrated by an automatic dewatering machine, embedded, sliced, and then stained with toluidine blue. The slices were soaked in APES (BL169A, Biosharp, China) and placed in an oven at 60 °C for 60 min to prevent slippage. After the slices were dewaxed to water, they were put into preheated 1 % toluidine blue solution (G1032, Servicebio, China), dyed at 56 °C for 20 min, and washed with distilled water. Then, the slices were soaked in 70 % alcohol for 1 min, differentiate with 95 % alcohol, dehydrated with gradient alcohol, transparent with xylene, and sealed with neutral gum. The numbers of positive neurons in the CA1 region of the hippocampus and prefrontal cortex were observed and counted under the microscope (BA400Digital, Panthera, China).

2.8. Transmission electron microscope

Hippocampal and prefrontal cortex tissues were prefixed with 3 % glutaraldehyde and 1 % osmium tetroxide, followed by step-by-step dehydration with acetone. After Ep812 was embedded, ultra-thin slices of about 60~90 nm were prepared by an ultra-thin slicing mechanism. Sections were stained with uranium acetate for 10–15 min, then with lead citrate for 1–2 min, at room temperature. The transmission electron microscope (JEM-1400FLASH, JEOL, Japan) was used to collect images.

2.9. Immunofluorescent staining

The paraffin sections of hippocampal tissue were dewaxed to water, the antigen was repaired with citrate buffer (PH 6.0), and the goat serum sealer was sealed at room temperature. The primary antibodies PSD95 (1: 200, 20665-1-AP, proteintech, China) and SYN (1: 100, 17785-1-AP, proteintech, China) were incubated at 4 °C overnight, and the secondary antibody FITC conjugated Goat Anti-Rabbit IgG (H + L) (1: 100, GB22303, Servicebio, China) was incubated at 37 °C for 30 min. Then, DAPI (ZLI-9557, ZSBIO, China) stained the nucleus at room temperature for 10 min, sealed with anti-fluorescence attenuation tablets, and observed by fluorescence

microscope (OlyVIA, OLYMPUS, JAPAN).

2.10. Transcriptome sequencing and analysis

Transcriptome sequencing was performed on mouse brain tissues in the control group, model group, and H-HLJDD group. Total RNA was extracted from each sample of the three groups, and the RNA concentration and purity were detected by agarose electrophoresis and Agilent 2100 Bioanalyzer. The mRNA with polyA structure in total RNA was enriched by Oligo (dT) magnetic beads, and the mRNA was interrupted to a fragment of about 300 bp in length. cDNA was synthesized using RNA as a template. After the completion of the library construction, PCR amplification was used to enrich the library fragments, and then the library was selected according to the fragment size, the library size was 450 bp. Then, the library was inspected by Agilent 2100 Bioanalyzer, and the total concentration and effective concentration of the library were detected. After RNA extraction, purification, and library construction, paired-end (PE) sequencing was performed using Next-Generation Sequencing (NGS) based on the Illumina sequencing platform. The Raw Data is filtered, and the filtered high-quality sequence is compared to the reference genome of the species. According to the comparison results, the expression amount of each gene was calculated. On this basis, the expression difference analysis, enrichment analysis, and cluster analysis of the samples were further carried out.

2.11. Western blot analysis

Total protein was extracted from the hippocampus and prefrontal cortex tissue with RIPA protein lysate (P0013, Beyotime, China) added with protease inhibitor (BL612A, Biosharp, China) and phosphatase inhibitor (BL615A, Biosharp, China), and normalized after quantification by BCA kit (P0009, Beyotime, China). The denatured proteins were separated by SDS-PAGE and transferred to PVDF membranes (Sigmaaldrich, USA). After being closed with 5 % skim milk for 2 h, primary antibodies RAS (1:1000; 3965, Cell Signaling Technology, USA), RAF1 (1:2000; 26863-1-AP, proteintech, China), MEK1/2 (1:2000; AF6385, affinity, China), *p*-MEK1/2 (1:1000; AF8035, affinity, China), ERK1/2 (1:2000; A16686, abclonal, China), *p*-ERK1/2 (1:2000; AP0472, abclonal, China), and β-actin (1:50000; AC026, abclonal, China) were incubated at 4 °C overnight. The second antibody Goat Anti-Rabbit IgG (H + L) HRP (1:5000; S0001, affbiotech, China) was incubated at room temperature for 2 h. The ECL developer (17046, zen-bio, China) and protein imaging system (5200 Multi, Tanon, China) visually analyze the proteins. The relative expression of the protein was calculated using β-actin as a reference.

2.12. Real-time quantitative polymerase chain reaction

Total RNA was extracted from mouse hippocampus and prefrontal cortex tissue using a total RNA extraction kit (19221ES50, YEASEN, China) and reversed into cDNA by PrimeScript RT reagent Kit (RR047A, Takara Bio, China), and then PCR reaction was performed with TB Green premix Ex *Taq*II (RR820A, TaKaRa, China) in a real-time fluorescent quantitative PCR assay system (QuantStudio TM3, ThermoFisher, USA). With β-actin as the reference gene, the gene expressions of RAS, RAF, MEK, and ERK were calculated by the $2^{-\triangle\triangle Ct}$ method. The sequence of primers used in the experiment was shown in Table 1.

2.13. Statistical analysis

The experimental data in this study were analyzed by SPSS 26.0 software. Data consistent with normal distribution were represented by mean ± standard deviation, and the difference among multiple groups was compared by one-way analysis of variance, $P < 0.05$ was considered statistically significant.

3. Results

3.1. Analysis of the main chemical components of HLJDD

The components in HLJDD were qualitatively analyzed by LC-MS/MS in positive-ion mode (Fig. 1A) and negative-ion mode (Fig. 1B), and twenty-two compounds were preliminarily identified in positive-ion mode (Table 2) and twenty-one compounds were identified in negative-ion mode (Table 3).

Table 1
The primer sequences used in the study.

Genes	Forward primer	Reverse primer
RAS	5′-GCATCCCCTACATTGAAACATC-3′	5′-CAATTTATGCTGCCGAATCTCA-3′
RAF	5′-AGGAGAACGAGGAGTCAGGCATC-3′	5′-TGCTGTCGGAGTCGGAGTCTG-3′
MEK	5′-AAAAGAGAAGGTGAAGAAGGGC-3′	5′-CAAATTCCTTCTTCCAGTTGCA-3′
ERK	5′-ATCTCAACAAAGTTCGAGTTGC-3′	5′-GTCTGAAGCGCAGTAAGATTTT-3′
β-actin	5′-CTACCTCATGAAGATCCTGACC-3′	5′-CACAGCTTCTCTTTGATGTCAC-3′

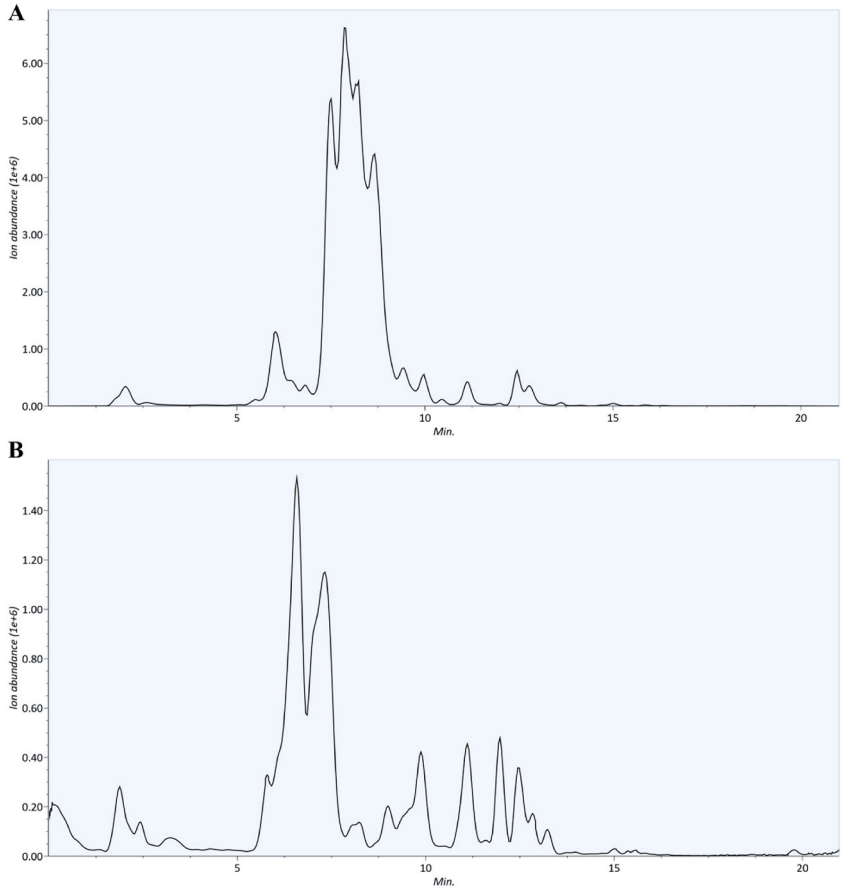

Fig. 1. Chromatogram of HLJDD. The positive-ion mode (A) and negative-ion mode (B) of HLJDD were detected by LC-MS/MS.

3.2. HLJDD improved the motor and learning ability of chronic alcohol-exposed mice

To explore the effects of HLJDD on mice with chronic alcohol exposure, mice were treated with low, medium, and high doses of HLJDD starting from the 8th day of alcohol exposure, and the weight of mice was monitored daily during the experiment (Fig. 2A). Compared with the control group, the weight of mice in the model group decreased significantly from day 10 until the end of the experiment ($P < 0.001$, Fig. 2A). And compared with the model group, L-HLJDD, M-HLJDD, and VB1 had no significant effect on the body weight of mice, and the weight of mice in the H-HLJDD group began to increase significantly from day 26 ($P < 0.05$, Fig. 2A). The behavior of mice was further tested, and the open field experiment results showed that compared with the control group, the total moving distance of mice in the chronic alcohol exposure model group was significantly reduced ($P < 0.001$, Fig. 2B and C), and compared with the model group, M-HLJDD, H-HLJDD, and VB1 could significantly increase the total moving distance of mice ($P < 0.001$, Fig. 2B and C), suggesting that HLJJD improved the movement disorder of mice with chronic alcohol exposure. Similarly, the results of the water maze experiment showed that compared with the control group, the total moving distance of mice in the model group to find the platform during the exploration experiment was significantly increased ($P < 0.001$, Fig. 2D and E), and compared with the model group, low, medium and high doses of HLJDD and VB1 could significantly reduce the total moving distance of mice to find the platform ($P < 0.001$, Fig. 2D and E), suggesting that HLJDD could significantly improve the cognitive function of mice.

3.3. HLJDD alleviates pathological damage of the hippocampus and prefrontal cortex of chronic alcohol-exposed mice

To further elucidate the effects of HLJDD on mice with chronic alcohol exposure, we collected brain tissues from mice and performed histopathological staining (Fig. 3A). The results showed that the cell layers in the cortex of the control group were arranged neatly and the morphology of neurons was normal. The pyramidal cell layers in the CA1 region of the hippocampus were arranged neatly, the cells were densely arranged, and no obvious glial cell proliferation and inflammatory cell infiltration were observed. Compared with the control group, the pyramidal cell layer of the hippocampal CA1 region was disordered in the model group, and the number of dark neurons in the hippocampal and prefrontal cortex increased significantly. L-HLJDD, M-HLJDD, H-HLJDD, and VB1 groups all reduced the degree of tissue lesions to some extent, and the H-HLJDD group had the most significant effect. In addition, the deposition of $A\beta_{1\text{-}42}$ in the CA1 region of the hippocampus was measured, and results showed that compared with the control group,

Table 2
Relevant mass spectral data of the components in HLJDD in the ESI positive-ion mode by LC-MS/MS.

Number	RT (min)	Precursor (*m/z*)	Reference (*m/z*)	Area	Adduct	Formula	Identification
1	5.46855	283.1209	283.12073	997699.75	$[M+H]^+$	$C_{15}H_{20}N_2O$	verruculotoxin
2	6.9954	145.0648	145.06479	222262.5781	$[M+H]^+$	$C_{10}H_8O$	1-Naphthol
3	1.764117	439.1398	439.14001	216048.6719	$[M+H]^+$	$C_{24}H_{22}O_8$	4-(3,7-dioxo-2-(propan-2-ylidene)-3,7,8,9-tetrahydro-2H-furo [2,3-f]chromen-9-yl)-2,6-dimethoxyphenyl acetate
4	11.57833	675.2606	675.26099	210560.2813	$[M+H]^+$	$C_{32}H_{44}O_{14}$	Jatrophane ester JE-C1
5	14.1707	323.0799	323.07999	201344.3438	$[M+H]^+$	$C_{14}H_{20}O_7$	Salidroside
6	12.53673	197.0055	197.00566	171509.8594	$[M+H]^+$	$C_6H_6O_6$	Aconitic Acid
7	2.038617	299.1276	299.12778	106353.2969	$[M+H]^+$	$C_{18}H_{18}O_4$	Enterolactone
8	11.42163	380.1124	380.11221	67083.32031	$[M+H]^+$	$C_{13}H_{21}N_3O_8S$	S-Lactoylglutathione
9	12.01133	339.1938	339.194	57971.31641	$[M+H]^+$	$C_{20}H_{28}O_3$	Cafestol
10	13.19635	315.1355	315.13568	56931.69141	$[M+H]^+$	$C_{17}H_{24}O_3$	shogaol
11	9.280534	333.0609	333.06079	54954.26563	$[M+H]^+$	$C_{16}H_{12}O_8$	Flavonol base + 4O, 1MeO
12	2.393	272.1281	272.12811	54708.08984	$[M+H]^+$	$C_{16}H_{14}O_3$	3-(alpha,alpha-dimethylallyl)psoralen
13	10.56608	478.2205	478.22021	53149.03125	$[M+H]^+$	$C_{22}H_{33}C_lO_8$	[6-acetyloxy-7-(chloromethyl)-7-hydroxy-1-(3-methylbutanoyloxy)-4a,5,6,7a-tetrahydro-1H-cyclopenta [c]pyran-4-yl]methyl 3-methylbutanoate
14	2.393	434.1801	434.17999	51885.26563	$[M+H]^+$	$C_{23}H_{23}N_5O_4$	N-(2-(2-(2-hydroxy-5-oxo-4,5-dihydro-3H-benzo[e][1,4] diazepin-3-yl)acetamido)ethyl)-1-methyl-1H-indole-2-carboxamide
15	14.092	359.0778	359.07803	45982.07031	$[M+H]^+$	$C_{20}H_{22}O_6$	11-methyl-2,7-dimethylidene-6,12-dioxo-5,14-dioxatricyclo [9.2.1.0,]tetradec-1 (13)-en-9-yl (2Z)-2-methylbut-2-enoate
16	2.432867	147.0665	147.06653	34456.67969	$[M+H]^+$	$C_7H_6N_4$	Phenyltetrazole
17	11.6175	659.203	659.20288	29438.79297	$[M+H]^+$	$C_{29}H_{32}O_{16}$	9-methoxy-7-[4-[3,4,5-trihydroxy-6-[[3,4,5-trihydroxy-6-(hydroxymethyl)oxan-2-yl]oxymethyl]oxan-2-yl] oxyphenyl]-[1,3]dioxolo [4,5-g]chromen-8-one
18	6.1385	435.1899	435.19	29046.30469	$[M+H]^+$	$C_{25}H_{26}N_2O_5$	2-(7,8-dimethoxy-4-methyl-2-oxo-2H-chromen-3-yl)-N-(1-isopropyl-1H-indol-4-yl)acetamide
19	11.81412	618.3823	618.38208	27089.9375	$[M+H]^+$	$C_{27}H_{48}N_6O_9$	deferrioxamine E
20	10.44958	400.1363	400.13599	26563.96875	$[M+H]^+$	$C_{17}H_{25}N_3O_4S_2$	Pesticide2_Alanycarb_C17H25N3O4S2_
21	14.01303	266.0578	266.05801	21587.85352	$[M+H]^+$	$C_{17}H_{15}NO_2$	Anonain
22	10.64372	344.1495	344.14923	20420.75586	$[M+H]^+$	$C_{19}H_{18}O_5$	7-[(E)-3-methyl-4-(4-methyl-5-oxo-2H-furan-2-yl)but-2-enoxy]chromen-2-one

the expression of $A\beta_{1\text{-}42}$ in the hippocampus of the model group was significantly increased, while M-HLJDD, H-HLJDD, and VB1 significantly decreased $A\beta_{1\text{-}42}$ expression in the model mice ($P < 0.001$, Fig. 3B and C). Then, the numbers of neurons in the hippocampus and prefrontal cortex were counted by Nissl staining, and the results showed that, compared with the control group, the numbers of neurons in the CA1 region of the hippocampus and prefrontal cortex of mice in the model group were significantly decreased, while L-HLJDD, M-HLJDD, H-HLJDD, and VB1 could significantly increase the numbers of positive neurons in the hippocampus and prefrontal cortex of model mice ($P < 0.001$, Fig. 3D and E). The ultrastructural changes of the hippocampus and prefrontal cortex were observed by transmission electron microscopy (Fig. 3F), and it was found that the morphology and structure of neurons in the control group were normal, chromatin was evenly distributed, and there were no significant changes occurred in mitochondria and rough endoplasmic reticulum. In the hippocampus and prefrontal cortex of the model group, the neurons were apoptotic, the cytoplasm was concentrated, the ribosome and mitochondria were aggregated, the cell size was reduced, the cell structure was more compact, heterochromatin gathered around the nuclear membrane, mitochondria were swollen, ridge lysis and breakage, the rough endoplasmic reticulum was expanded, and the space between the two layers of the cystic structure was widened. L-HLJDD, M-HLJDD, H-HLJDD, and VB1 all improved the pathological damage of the hippocampus and prefrontal cortex to a certain extent, and H-HLJDD had the best effect, followed by M-HLJDD. Further detection of synapse-related proteins in the hippocampus showed that the expressions of PSD95 and SYN were significantly decreased in the model group compared with the control group, and M-HLJDD, H-HLJDD, and VB1 significantly increased the expressions of PSD95 and SYN in the hippocampus of the model group compared with the model group ($P < 0.05$, Fig. 4A–C). All these results suggested that HLJDD could improve the prefrontal cortex and hippocampal damage of chronic alcohol-exposed mice.

3.4. Transcriptome sequencing analysis of the effects of HLJDD on chronic alcohol-exposed mice

The above studies have confirmed that HLJDD could significantly improve the neuropathological injury and behavioral disorders of chronic alcohol-exposed mice. To further elucidate its mechanism, transcriptome sequencing was performed on the brain tissues of mice in the control group, model group, and H-HLJDD group. According to the comparison results, the expression amount of each gene was calculated, and the expression difference analysis, cluster analysis, and enrichment analysis were carried out for each sample. The density map and violin map of the FPKM density distribution of each sample showed the characteristic statistical results of gene expression in each sample (Fig. 5A and B). Before the differential expression analysis, the Pearson correlation coefficient was used to

Table 3
Relevant mass spectral data of the components in HLJDD in the ESI negative-ion mode by LC-MS/MS.

Number	RT (min)	Precursor (*m/z*)	Reference (*m/z*)	Area	Adduct	Formula	Identification
1	5.3006	391.1763	391.17621	997016.3125	[M − H]⁻	$C_{21}H_{28}O_7$	6-formyl-10-(hydroxymethyl)-5-methoxy-3-methylidene-2-oxo-2H,3H,3aH,4H,5H,8H,9H,11aH-cyclodeca [*b*] furan-4-yl 2-methylbutanoate
2	10.4242	477.1967	477.19644	514369.375	[M − H]⁻	$C_{23}H_{26}O_{11}$	calceolarioside A
3	11.97095	583.2045	583.20441	487432.4688	[M − H]⁻	$C_{26}H_{34}O_{12}$	Tanegoside (Not validated)
4	13.27337	327.1714	327.17142	342479.4063	[M − H]⁻	$C_{19}H_{24}N_2O_3$	Labetalol
5	7.406867	355.1122	355.11218	271536.4063	[M − H]⁻	$C_{19}H_{20}N_2O_3S$	Pioglitazone
6	6.934717	481.116	481.116	191539.5625	[M − H]⁻	$C_{25}H_{22}O_{10}$	Silibinin
7	6.579733	355.1175	355.11761	177273.0156	[M − H]⁻	$C_{20}H_{20}O_6$	Flavanone base + 4O, 1 Prenyl
8	3.4759	405.1553	405.15549	164326.4688	[M − H]⁻	$C_{20}H_{24}O_6$	Lariciresinol
9	6.619233	401.1607	401.16058	160747.9844	[M − H]⁻	$C_{22}H_{26}O_7$	gmelinol
10	1.759333	473.1819	473.1817	130195.6641	[M − H]⁻	$C_{25}H_{30}O_9$	[(4R,6aR,9S,9aR,9bR)-9-methyl-3,6-dimethylidene-2,8-dioxo-3a,4,5,6a,7,9,9a,9b-octahydroazuleno [4,5-*b*]furan-4-yl] (E)-4-hydroxy-2-[[(E)-4-hydroxy-2-methylbut-2-enoyl]oxymethyl]but-2-enoate
11	3.435733	413.1568	413.15656	114865.5469	[M − H]⁻	$C_{18}H_{26}N_2O_9$	2-amino-5-[2-[[2,3-dihydroxy-2-(1-hydroxyethyl) butanoyl]oxymethyl]-4-hydroxyanilino]-5-oxopentanoic acid
12	3.276083	557.2457	557.24573	103122.1563	[M − H]⁻	$C_{33}H_{35}FN_2O_5$	Atorvastatin
13	6.264917	327.0863	327.086	97617.39844	[M − H]⁻	$C_{18}H_{16}O_6$	5-hydroxy-3,7-dimethoxy-2-(4-methoxyphenyl)-4H-chromen-4-one
14	12.91845	327.2304	327.23019	84996.02344	[M − H]⁻	$C_{18}H_{32}O_5$	(10E,15Z)-9,12,13-trihydroxyoctadeca-10,15-dienoic acid
15	2.476467	299.1042	299.10449	59555.80859	[M − H]⁻	$C_{16}H_{12}O_6$	tectorigenin
16	13.27337	283.1777	283.17767	56273.26172	[M − H]⁻	$C_{17}H_{16}O_4$	3,9-Dimethoxypterocarpan
17	8.87895	407.1855	407.1853	52110.48438	[M − H]⁻	$C_{25}H_{28}O_5$	Licodione base + 2 Prenyl
18	2.556117	343.0808	343.08099	46265.07422	[M − H]⁻	$C_{18}H_{16}O_7$	5,7-dihydroxy-3,6-dimethoxy-2-(4-methoxyphenyl)-4H-chromen-4-one
19	12.83507	431.1263	431.1265	35559.19141	[M − H]⁻	$C_{21}H_{20}O_{10}$	5,7-dihydroxy-2-(4-hydroxyphenyl)-6-[3,4,5-trihydroxy-6-(hydroxymethyl)oxan-2-yl]chromen-4-one
20	13.98717	521.1975	521.19751	28343.31445	[M − H]⁻	$C_{24}H_{26}O_{13}$	salviaflaside
21	13.43037	483.2962	483.29633	21398.61523	[M − H]⁻	$C_{26}H_{44}O_8$	(2R,3S,4S,5S,6R)-2-[[7-hydroxy-4-[(Z)-5-hydroxy-3-methylpent-3-enyl]-4a,8,8-trimethyl-3-methylidene-2,4,5,6,7,8a-hexahydro-1H-naphthalen-2-yl]oxy]-6-(hydroxymethyl)oxane-3,4,5-triol

represent the correlation of gene expression levels among samples (Fig. 5C). The correlation coefficient of all samples was close to 1, indicating the high similarity of expression patterns among samples, which proved the high reliability of this experiment and reasonable sample selection. Then, DESeq was used to analyze the difference in gene expression, and $|\log2FoldChange| > 1$ and $P < 0.05$ were used for screening. The volcano map of differentially expressed genes was drawn using the R language ggplots2 software package (Fig. 5D). The statistical results of differentially expressed genes among different groups found that, compared with the control group, 62 genes were up-regulated and 15 genes were down-regulated in the brain tissue of chronic alcohol-exposed mice, and 23 genes were up-regulated and 108 genes were down-regulated in the H-HLJDD group (Fig. 5E). And compared with the model group, there were 23 up-regulated genes and 56 down-regulated genes in the H-HLJDD group (Fig. 5E). The R language Pheatmap software package was used to conduct bidirectional cluster analysis on the union of differential genes and samples of all comparison groups. Clustering was carried out according to the expression level of the same gene in different samples and the expression pattern of different genes in the same sample (Fig. 5F). In addition, the Vann diagram was drawn using the R language ggvenn package to obtain the intersection of differentially expressed genes (Fig. 5G), the same differentially expressed genes between "control vs model" and "model group vs H-HLJDD" mainly include "Gucy1a2, Zfp677, Slfn9, Il1rapl2, Ces2g, BC024063, Zfp97, Macc1, Gm7072, Wfikkn1, Bnipl".

Functional enrichment analysis of differentially expressed genes was further performed. The GO enrichment analysis results of

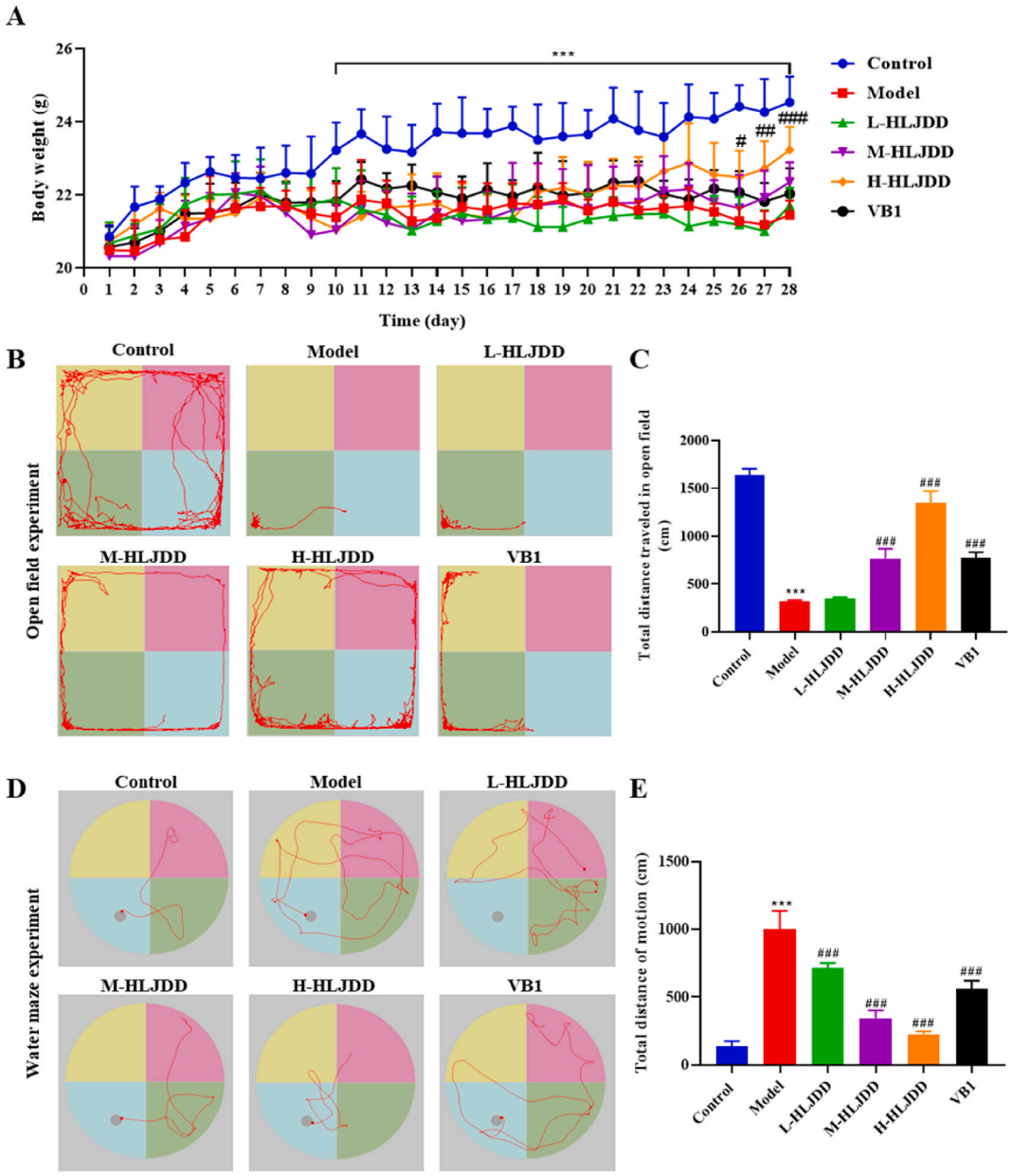

Fig. 2. Effects of HLJDD on the behavior of chronic alcohol-exposed mice. A: Weight monitoring of mice during the experiment. **B:** The movement track of mice in the open field experiment. **C:** Total movement distance of mice in open field experiment. **D:** Motion track of Morris water maze experiment. **E:** The distance the mice found the platform to move in the water maze experiment. $^{*}P < 0.05$, $^{**}P < 0.01$, $^{***}P < 0.001$, compared with the control group. $\#P < 0.05$, $\#\#P < 0.01$, $\#\#\#P < 0.001$, compared with the model group.

differentially expressed genes were classified according to molecular function (MF), biological process (BP), and cellular component (CC), and the top 10 GO term entries with the lowest *P*-value, that is, the most significant enrichment, were selected from each GO classification for display (Fig. 6A). In addition, according to the KEGG enrichment analysis results of differentially expressed genes, the first 30 pathways with the lowest *P*-value were selected for display (Fig. 6B). The KEGG enrichment results were further statistically analyzed, and the intersection between each group was plotted (Fig. 6C). 23 KEGG pathways intersected between "control vs model", "model vs H-HLJDD", and "control vs H-HLJDD", including: "Herpes simplex virus 1 infection, Neuroactive ligand-receptor interaction, Nicotine addiction, Long-term depression, Ras signaling pathway, etc.". Among them, the Ras signaling pathway is thought to be involved in various disease processes.

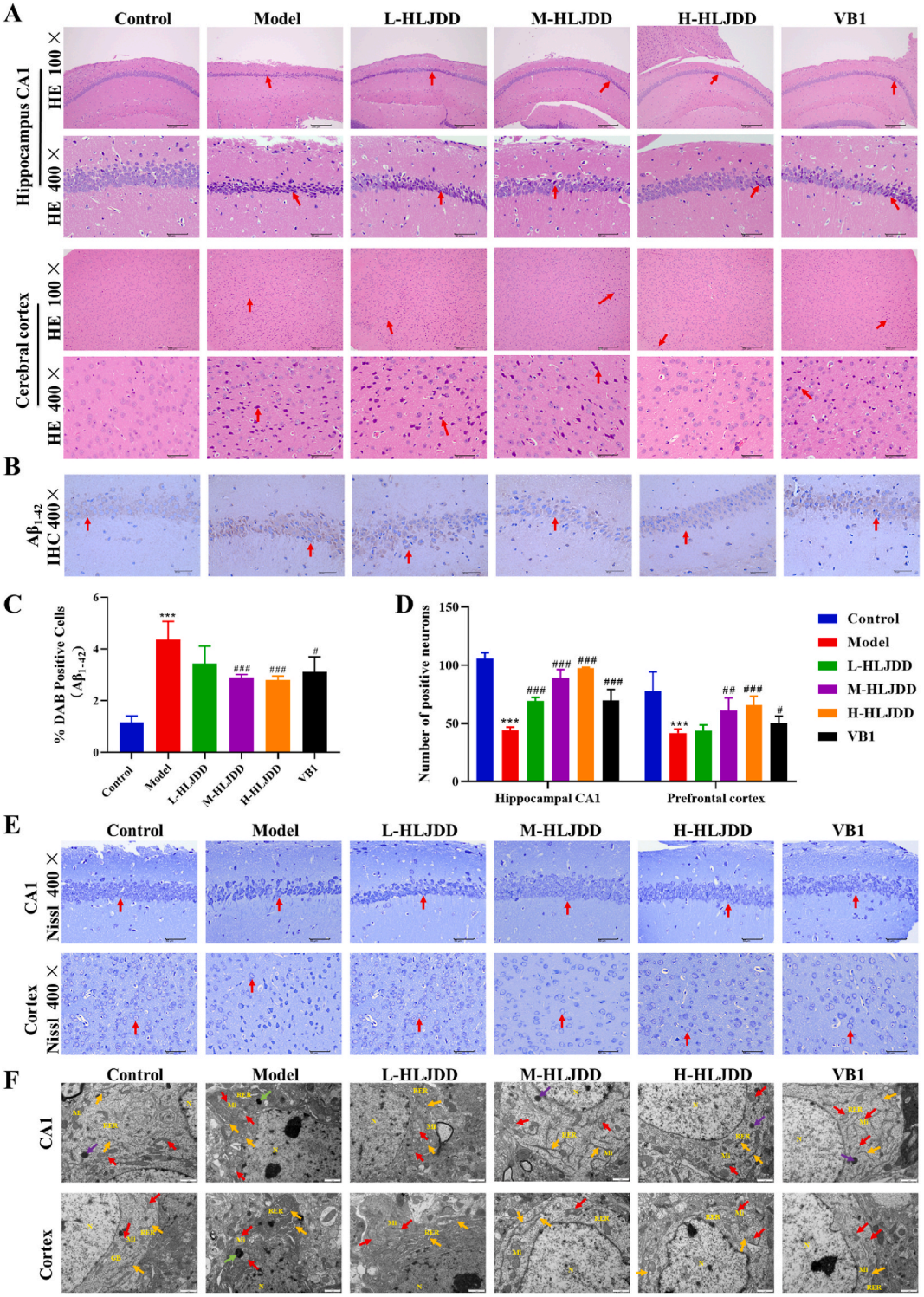

(caption on next page)

Fig. 3. Effects of HLJDD on pathological changes of the hippocampus and prefrontal cortex of chronic alcohol-exposed mice. A: HE staining of the hippocampus and prefrontal cortex. The red arrows show the diseased dark neurons. B: Immunohistochemical staining of $A\beta_{1\text{-}42}$ in hippocampal tissue. Red arrows indicate positive staining. **C:** Statistical result of the percentage of $A\beta_{1\text{-}42}$ positive cells in hippocampal tissue. **D:** Statistical results of the number of positive neurons in the hippocampus and prefrontal cortex in Nissl staining. **E:** The survival of neurons in the hippocampus and prefrontal cortex was observed with Nissl staining. Red arrows indicate positive neurons. **F:** Microscopic pathological changes of neurons in the hippocampus and prefrontal cortex were observed by transmission electron microscopy. Nucleus (N), mitochondria (Mi), rough endoplasmic reticulum (RER). Red arrows represent neurons with normal or swollen mitochondria, yellow arrows represent the rough endoplasmic reticulum, purple arrows represent primary lysosomes, and green arrows represent secondary lysosomes. $^{*}P < 0.05$, $^{**}P < 0.01$, $^{***}P < 0.001$, compared with the control group. $\#P < 0.05$, $\#\#P < 0.01$, $\#\#\#P < 0.001$, compared with the model group. (For interpretation of the references to color in this figure legend, the reader is referred to the Web version of this article.)

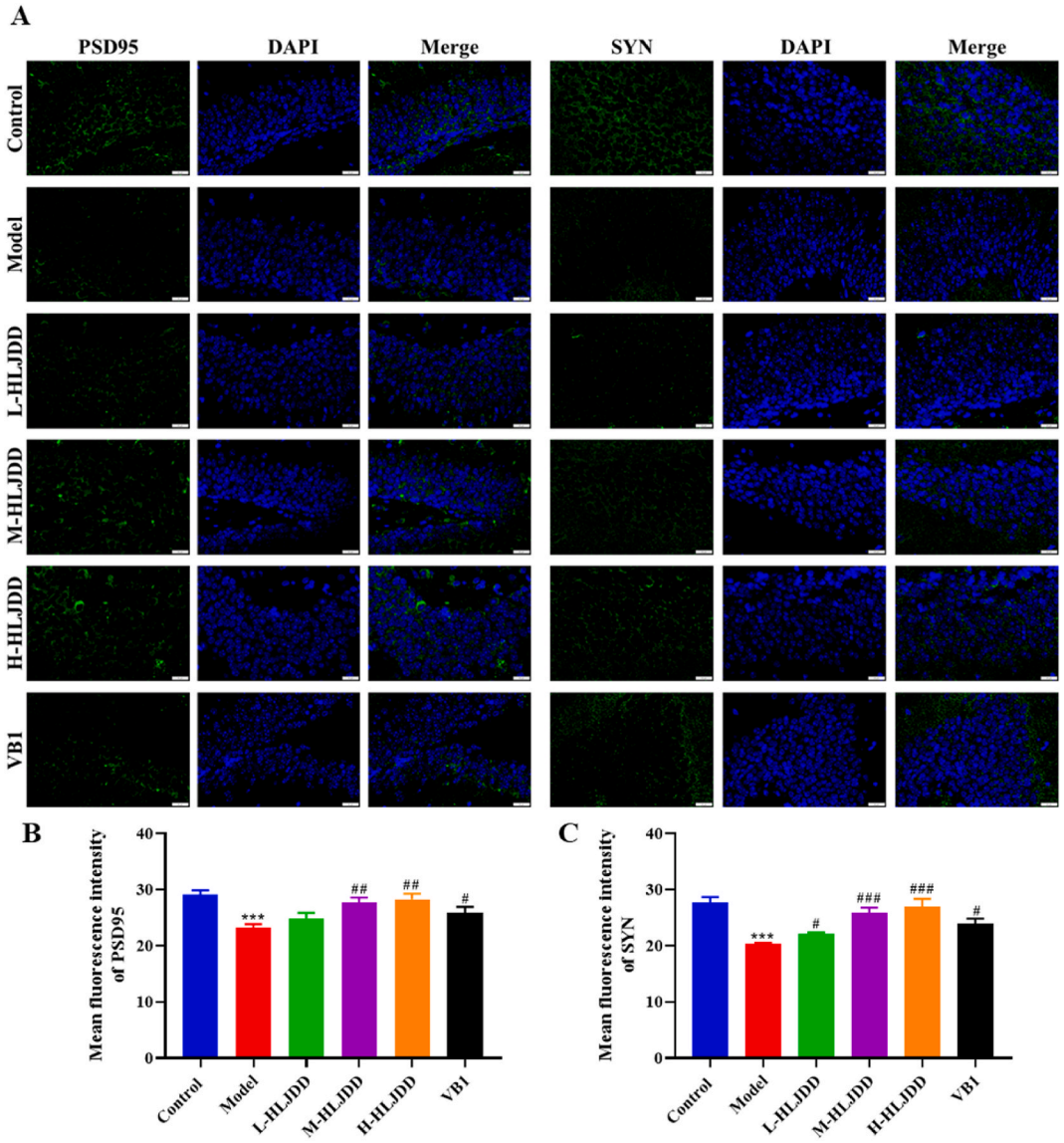

Fig. 4. Effects of HLJDD on synaptic remodeling in mice with chronic alcohol exposure. A: The expression of synaptic remodeling-related protein PSD95 and SYN in the hippocampus was detected by immunofluorescence. **B:** Statistical results of mean fluorescence intensity of PSD95 in the hippocampus. **C:** Statistical result of mean fluorescence intensity of SYN in the hippocampus. $^{*}P < 0.05$, $^{**}P < 0.01$, $^{***}P < 0.001$, compared with the control group. $\#P < 0.05$, $\#\#P < 0.01$, $\#\#\#P < 0.001$, compared with the model group.

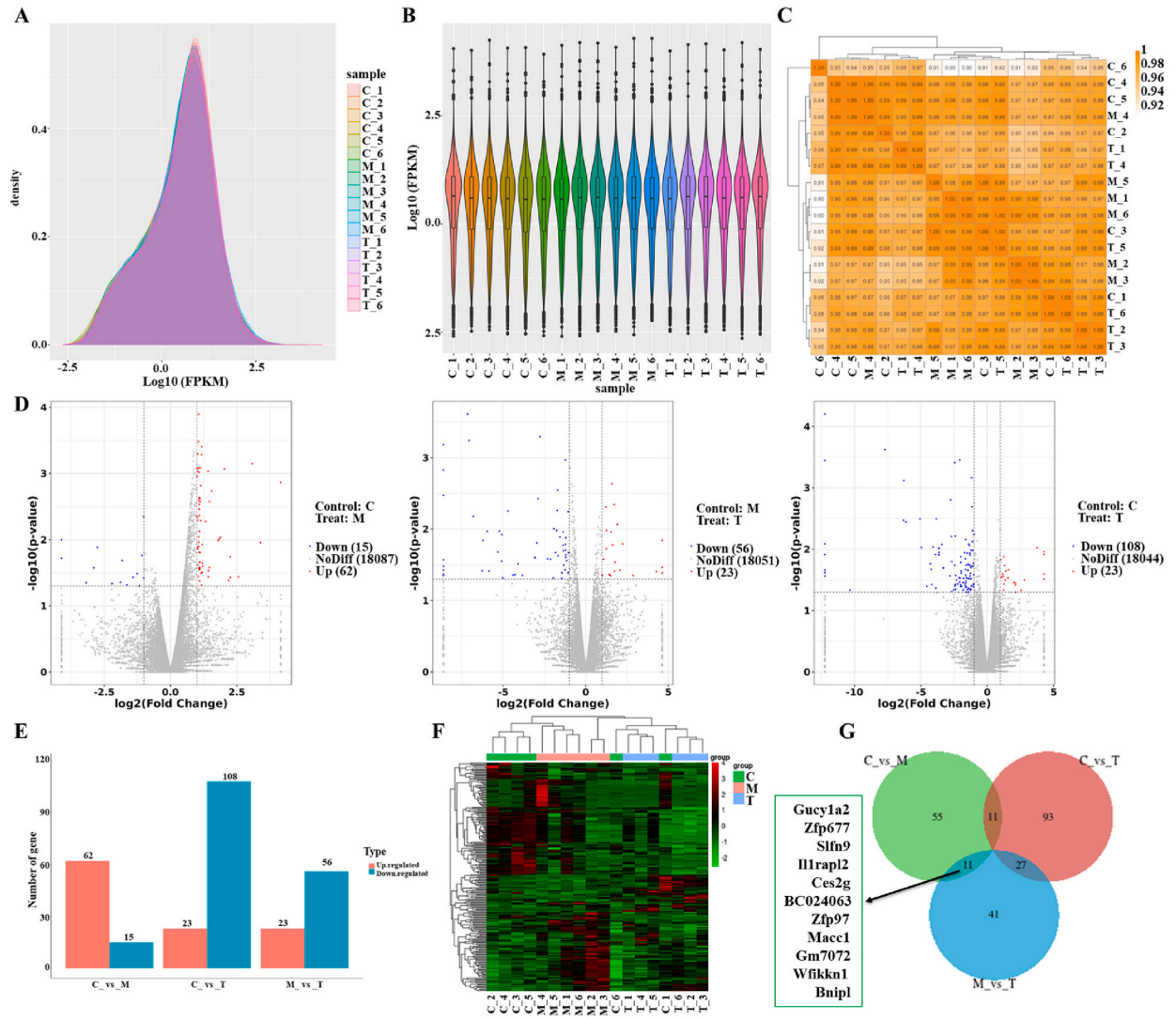

Fig. 5. Analysis of differentially expressed genes in brain tissue of chronic alcohol-exposed mice by HLJDD. A. FPKM density distribution was used to investigate the expression patterns of all genes in the samples. The horizontal coordinate is the log 10(FPKM) value of the gene, and the vertical coordinate is the gene distribution density corresponding to the expression amount. **B:** Violin diagram of FPKM density distribution. The horizontal line in the middle of the box is the median, the upper and lower edges of the box are 75 %, the upper and lower limits are 90 %, and the outer shape is the kernel density estimate. **C:** Pearson correlation coefficient represents the correlation of gene expression levels between samples. **D:** The volcano map of differentially expressed genes, from left to right, is the control and model group, the model and treatment group, and the control and treatment group, respectively. **E.** Statistical results of expression difference analysis. **F:** Clustering heat map of differentially expressed genes. **G:** Venn map of differentially expressed genes. C: control; M: model; T: H-HLJDD.

3.5. HLJDD regulated the RAS-RAF-MEK-ERK pathway in mice with chronic alcohol exposure

To verify whether the RAS-RAF-MEK-ERK pathway was involved in HLJDD alleviating neuropathological injury in mice with chronic alcohol exposure, the protein and gene expressions of the RAS-RAF-MEK-ERK pathway were detected. WB results showed that compared with the control group, the protein expression levels of RAS, RAF, *p*-MEK/MEK, and *p*-ERK/ERK both in the hippocampus and prefrontal cortex tissue of the model group were significantly increased, while M-HLJDD, H-HLJDD, and VB1 significantly reduced their expression levels in the model group ($P < 0.05$, Fig. 7A and B). The results of RT-PCR were consistent with the results of protein detection, showing that the gene expression levels of RAS, RAF, MEK, and ERK in the hippocampus and prefrontal cortex tissue of mice in the model group were significantly increased, and these increased gene expressions were significantly decreased by M-HLJDD, H-HLJDD and VB1 ($P < 0.05$, Fig. 7C). It was suggested that HLJDD could regulate the RAS-RAF-MEK-ERK pathway in mice with chronic alcohol exposure.

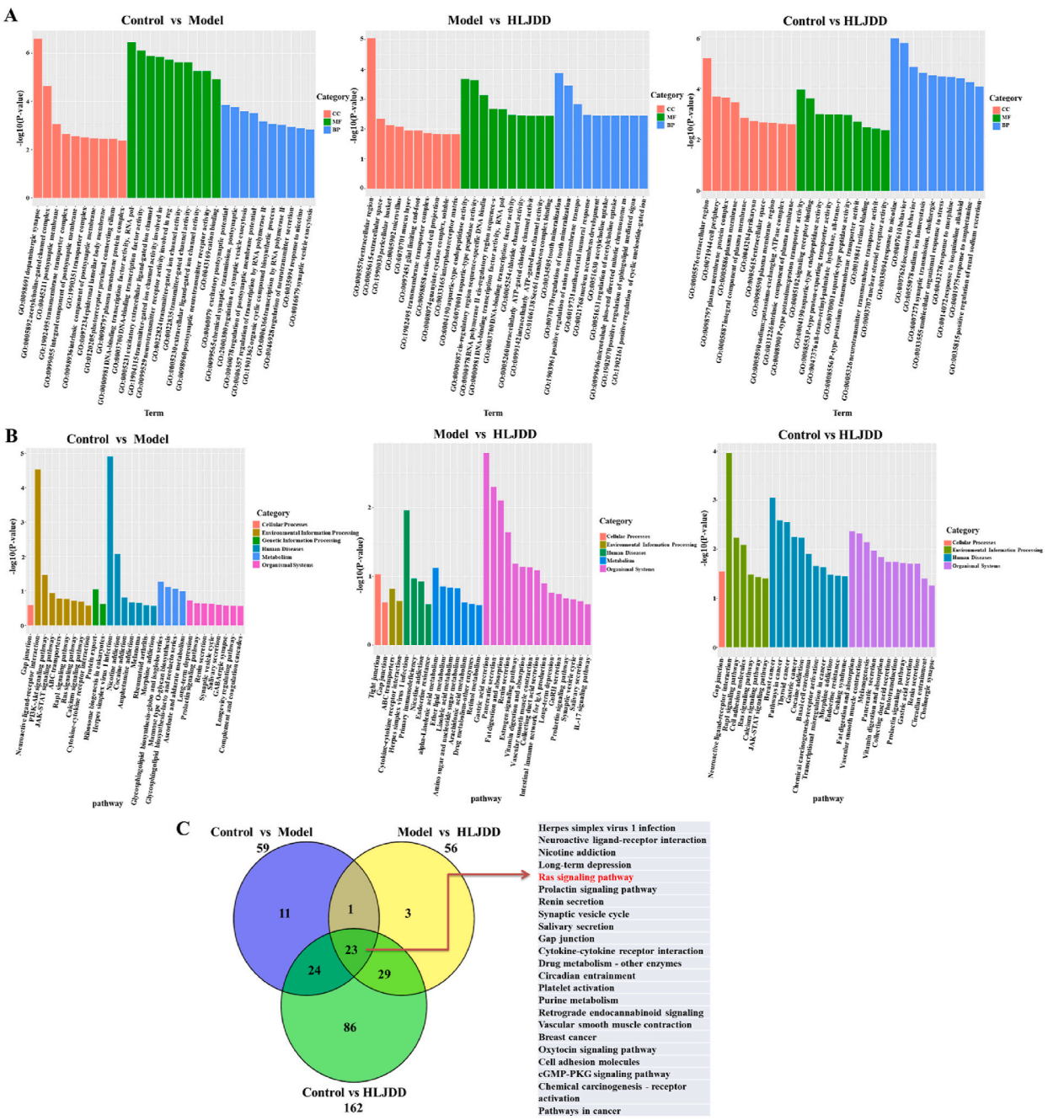

Fig. 6. GO and KEGG enrichment analysis. A: GO statistical histogram of differential genes. **B:** KEGG statistical histogram of differential genes. **C:** Venn map of the intersection of KEGG enrichment pathways. C: control; M: model; T: H-HLJDD.

4. Discussion

Long-term excessive drinking is easy to cause serious multi-organ, mental, and nervous system damage, especially serious damage to the cerebral cortex, which can cause mental disorders, resulting in alcoholic encephalopathy [16]. HLJDD is a classic Chinese herbal compound for clearing heat and detoxification, which has many pharmacological effects [17]. This study found that HLJDD significantly reversed weight loss, motor and cognitive dysfunction in chronic alcohol-exposed mice, as well as reversed $A\beta_{1\text{-}42}$ deposition, improved pathological damage in the hippocampus and prefrontal cortex, and increased the expressions of synaptic proteins SDP95 and SYN. Transcriptome sequencing and subsequent validation experiments indicated that HLJDD may ameliorate the neuropathological injury of chronic alcohol-exposed mice by regulating the RAS-RAF-MEK-ERK pathway.

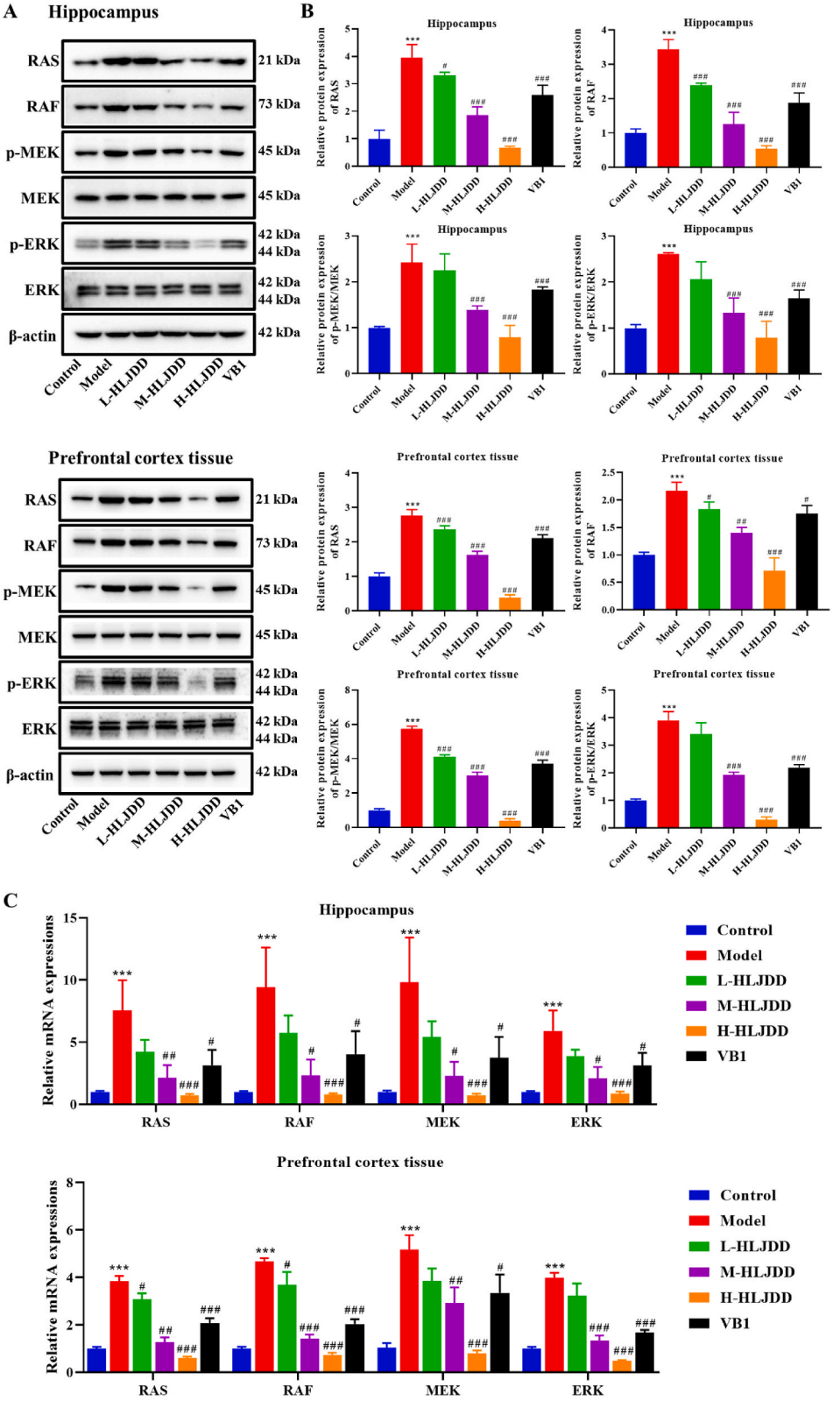

(caption on next page)

Fig. 7. Effects of HLJDD on the RAS-RAF-MEK-ERK pathway in mice with chronic alcohol exposure. A: The protein expressions of RAS, RAF, *p*-MEK, MEK, *p*-ERK, and ERK in mouse hippocampus and prefrontal cortex tissue were detected by WB. **B:** Statistical results of RAS, RAF, *p*-MEK/MEK, and *p*-ERK/ERK relative protein expression. **C:** The gene expression levels of RAS, RAF, MEK, and ERK were detected by RT-PCR. $^{*}P < 0.05$, $^{**}P < 0.01$, $^{***}P < 0.001$, compared with the control group. $\#P < 0.05$, $\#\#P < 0.01$, $\#\#\#P < 0.001$, compared with the model group.

Chronic alcoholic encephalopathy is caused by chronic drinking, alcohol provides only calories, and does not contain vitamins and minerals. Long-term alcohol consumption can cause gastrointestinal dysfunction, reduce vitamin intake, resulting in reduced thiamine phosphate, severe deficiency of nerve energy supply substances, and eventually brain dysfunction [18–20]. Studies have shown that chronic alcohol exposure altered gene expression in brains and pathways associated with multiple neurodegenerative diseases such as AD and Parkinson's disease (PD) [21]. In addition, chronic ethanol exposure affected anxiety-like behavior and basic synaptic function as well as neuronal excitability in brain regions of the prefrontal cortex and expanded amygdala [22]. This study showed that behavioral cognitive function was impaired, the hippocampus and prefrontal cortex were pathologically damaged, the expression of $A\beta_{1\text{-}42}$ in the hippocampus was significantly increased, and the number of neurons and the expression of synapse-related proteins were significantly decreased in chronic alcohol-exposed mice, suggesting that chronic alcohol exposure caused neurobehavioral impairment.

As a representative prescription for clearing heat and detoxification, HLJDD is a reasonable combination of *Coptis chinensis* Franch., *Scutellaria baicalensis* Georgi, *Phellodendron chinense* Schneid. and *Gardenia jasminoides J.* Ellis, which makes the efficacy stronger [23]. Modern pharmacological studies have shown that HLJDD can effectively improve the learning and memory ability of diabetic encephalopathy mice and prevent neurodegeneration [24]. HLJDD can also alleviate depression-like behavior in colitis mice by inhibiting the Trem2/Dap12 pathway in microglia, which is conducive to precise treatment [25]. As a traditional Chinese medicine, the application of HLJDD in the field of neurobehavioral injury is relatively rare. This study combined traditional Chinese medicine with modern medical theory to investigate its role in the field of neurobiology, and the results showed that HLJDD significantly improved the behavior and cognitive impairment of chronic alcohol-exposed mice. In addition, HLJDD improved hippocampal and prefrontal cortex damage and reduced $A\beta_{1\text{-}42}$ deposition in hippocampal tissues of mice with chronic alcohol exposure. Aβ is a protein strongly associated with cellular aging and oxidative damage, and is a central component of the characteristic deposits that make up age plaques in the brains of AD [26]. Previous studies have found that depression and cognitive dysfunction in elderly patients are correlated with changes in serum and cerebrospinal fluid $A\beta_{1\text{-}42}$ concentration [27]. HLJDD could improve Aβ toxicity in mouse models and play a good therapeutic role in AD [28]. It has also been confirmed that HLJDD could improve gene expression patterns in the hippocampus and cerebral cortex of senescence-accelerated mice [29]. Our study found that HLJDD significantly promoted an increase in the number of neurons in the hippocampus and prefrontal cortex and improve pathological damage in chronic alcohol-exposed mice. In addition, HLJDD was found to promote the expressions of PSD95 and SYN in the hippocampus of chronic alcohol-exposed mice. PSD95 is a very important scaffold protein in mature glutamate synapses, which supports the maturation of synapses and plays a very important role in the strength and plasticity of synapses, and is considered as a landmark protein for evaluating synaptic strength [30]. SYN, also known as major synaptic vesicle protein p38, interacts with the basic synaptic vesicle protein to regulate synaptic vesicle endocytosis [31]. The present study observed that HLJDD reversed the decline in PSD95 and SYN expression caused by chronic alcohol exposure, inferring that HLJDD has a significant role in promoting the repair, maturation, and function of synapses in the damaged area, providing a new strategy for the treatment of neurobehavioral injury.

The differentially expressed genes after chronic alcohol exposure and HLJDD treatment were analyzed by transcriptome sequencing, and their functional enrichment analysis was conducted. It was found that the RAS signaling pathway may be involved in brain injury caused by chronic alcohol exposure and the mitigation effect of HLJDD. RAS pathway is one of the important intracellular signaling mechanisms, regulating cellular processes, and is also the main intersection of many signal transduction pathways, acting through the downstream effector MEK/ERK [32,33]. When RAS is stimulated by extracellular signals, it is transformed into active RAS, which then activates RAF1, and RAF1 can phosphorylate and activate MEK, and *p*-MEK further phosphorylates ERK1/2 [34]. This activation process transfers extracellular signals through the cell membrane and cytoplasm to the nucleus to regulate the cell cycle and the physiological and pathological processes of cells [35]. Studies have shown that the ERK pathway is involved in the regulation of tight junction protein expression and is closely related to blood-brain barrier permeability [36]. ERK showed continuous overactivation during brain trauma, and its expression duration was significantly prolonged [37,38]. And RAS-RAF-MEK-ERK signal transduction pathway composed of RAS and downstream RAF-MEK plays an important role in the development and function of neurons [39]. Reducing RAS expression, weakening the phosphorylation levels of ERK, and inhibiting the activation of astrocytes and the occurrence and development of inflammation, can reduce nerve cell apoptosis, improve nerve function deficit, and alleviate brain injury [40,41]. In addition, studies have shown that natural products treat neurodegenerative diseases through the RAS/RAF/MAPK pathway [42]. Although the role of the RAS/RAF/MEK/ERK pathway in a variety of diseases has been extensively studied, its role in neurobehavioral impairment caused by chronic alcohol exposure and its regulation by HLJDD are still relatively new areas of research. This study further confirmed that chronic alcohol exposure activated the RAS-RAF-MEK-ERK pathway, and HLJDD significantly inhibited its activation, suggesting that HLJDD might alleviate the neuropathological damage caused by chronic alcohol exposure through the RAS-RAF-MEK-ERK pathway.

In conclusion, HLJDD significantly improved motor cognition ability, reduced $A\beta_{1\text{-}42}$ deposition, and increased the number of neurons in the hippocampus and prefrontal cortex in chronic alcohol-exposed mice. Also, HLJDD increased the expression of synaptic proteins PSD95 and SYN in the hippocampus of chronic alcohol-exposed mice. Transcriptome sequencing analysis showed that the ameliorating effect of HLJDD on brain injury in chronic alcohol exposure may be related to the RAS pathway. Further experiments

demonstrated that HLJDD significantly reduced the protein and gene expressions of the RAS-RAF-MEK-ERK pathway in brain tissue of chronic alcohol-exposed mice, suggesting that HLJDD improved neurobehavioral damage in mice with chronic alcohol exposure by regulating the RAS-RAF-MEK-ERK pathway (Supplementary Fig. 1). In general, although HLJDD has been widely used in the clinical practice of traditional Chinese medicine, this study confirmed its association with the RAS-RAF-MEK-ERK pathway, and in-depth analyzed the pharmacological and molecular biological mechanisms of HLJDD, especially its association with key signaling pathways in modern biomedicine. It has laid the foundation for promoting the integration and development of traditional Chinese medicine and modern biomedicine. However, it is worth noting that the number of animals in this study is limited, which may have some limitations. In order to further apply the research results, preclinical and clinical experiments with a larger sample size are still needed.

Funding

This work was supported by the Bijie City Science and Technology Bureau joint fund project [2023] No. 58.

Ethical statement

All operations were approved by the Experimental Animal Ethics Committee of Chengdu University of Traditional Chinese Medicine (No. 2022-59).

Data availability statement

The datasets used and/or analyzed during the current study are available from the corresponding author on reasonable request.

CRediT authorship contribution statement

Yun Chen: Writing – original draft, Data curation, Conceptualization. **Lianyan Jiang:** Writing – review & editing, Data curation. **Mao Li:** Writing – review & editing, Data curation. **Yuling Shen:** Writing – review & editing, Data curation. **Shanyu Liu:** Writing – review & editing, Data curation. **Dongdong Yang:** Writing – review & editing, Writing – original draft, Conceptualization.

Declaration of competing interest

The authors declare that they have no known competing financial interests or personal relationships that could have appeared to influence the work reported in this paper.

Appendix A. Supplementary data

Supplementary data to this article can be found online at https://doi.org/10.1016/j.heliyon.2024.e29556.

References

[1] R. Sircar, Behavioral changes and dendritic remodeling of hippocampal neurons in adolescent alcohol-treated rats, Advances in drug and alcohol research 3 (2023) 11158.
[2] S. De Santis, A. Cosa-Linan, R. Garcia-Hernandez, L. Dmytrenko, L. Vargova, I. Vorisek, et al., Chronic alcohol consumption alters extracellular space geometry and transmitter diffusion in the brain, Sci. Adv. 6 (2020) eaba0154.
[3] C. Kramarz, E. Murphy, M.M. Reilly, A.M. Rossor, Nutritional peripheral neuropathies, J. Neurol. Neurosurg. Psychiatr. 95 (2023) 61–72.
[4] S. Baltrusch, The role of Neurotropic B vitamins in nerve regeneration, BioMed Res. Int. 2021 (2021) 9968228.
[5] B. Le Daré, V. Lagente, T. Gicquel, Ethanol and its metabolites: update on toxicity, benefits, and focus on immunomodulatory effects, Drug Metab. Rev. 51 (2019) 545–561.
[6] S.K. Kunutsor, A. Bhattacharjee, M.A. Connelly, S.J.L. Bakker, R.P.F. Dullaart, Alcohol consumption, high-density lipoprotein particles and subspecies, and risk of cardiovascular disease: findings from the PREVEND prospective study, Int. J. Mol. Sci. 25 (2024).
[7] S.M. de la Monte, J.J. Kril, Human alcohol-related neuropathology, Acta Neuropathol. 127 (2014) 71–90.
[8] J. Shang, Q. Li, T. Jiang, L. Bi, Y. Lu, J. Jiao, et al., Systems pharmacology, proteomics and in vivo studies identification of mechanisms of cerebral ischemia injury amelioration by Huanglian Jiedu Decoction, J. Ethnopharmacol. 293 (2022) 115244.
[9] J. Liang, Y. Huang, Z. Mai, Q. Zhan, H. Lin, Y. Xie, et al., Integrating network pharmacology and experimental validation to decipher the mechanism of action of huanglian Jiedu decoction in treating atherosclerosis, Drug Des. Dev. Ther. 15 (2021) 1779–1795.
[10] L.N. Wang, X.R. Gu, N. Si, H.J. Wang, Y.Y. Zhou, B.L. Bian, et al., [Biomarkers related to cognitive dysfunction in APP/PS1 mice based on non-targeted metabonomics and intervention mechanism of Huanglian Jiedu Decoction], Zhongguo Zhong yao za zhi = China journal of Chinese materia medica 47 (2022) 6117–6126.
[11] X. Gu, J. Zhou, Y. Zhou, H. Wang, N. Si, W. Ren, et al., Huanglian Jiedu decoction remodels the periphery microenvironment to inhibit Alzheimer's disease progression based on the "brain-gut" axis through multiple integrated omics, Alzheimer's Res. Ther. 13 (2021) 44.
[12] H. Liu, X. Chen, Y. Liu, C. Fang, S. Chen, Antithrombotic effects of Huanglian Jiedu decoction in a rat model of ischaemia-reperfusion-induced cerebral stroke, Pharmaceut. Biol. 59 (2021) 823–827.
[13] T.E. Thiele, M. Navarro, "Drinking in the dark" (DID) procedures: a model of binge-like ethanol drinking in non-dependent mice, Alcohol (Fayetteville, N.Y.) 48 (2014) 235–241.

[14] N. Huynh, N.M. Arabian, L. Asatryan, D.L. Davies, Murine drinking models in the development of pharmacotherapies for alcoholism: drinking in the dark and two-bottle choice, J. Vis. Exp. 7 (2019), https://doi.org/10.3791/57027.
[15] Y. Cai, J. Wen, S. Ma, Z. Mai, Q. Zhan, Y. Wang, et al., Huang-lian-jie-du decoction attenuates atherosclerosis and increases plaque stability in high-fat diet-induced ApoE(-/-) mice by inhibiting M1 macrophage polarization and promoting M2 macrophage polarization, Front. Physiol. 12 (2021) 666449.
[16] K.N. Nwachukwu, D.M. King, K.L. Healey, H.S. Swartzwelder, S.A. Marshall, Sex-specific effects of adolescent intermittent ethanol exposure-induced dysregulation of hippocampal glial cells in adulthood, Alcohol (Fayetteville, N.Y.) 100 (2022) 31–39.
[17] R. Tian, X. Liu, L. Jing, L. Yang, N. Xie, Y. Hou, et al., Huang-Lian-Jie-Du decoction attenuates cognitive dysfunction of rats with type 2 diabetes by regulating autophagy and NLRP3 inflammasome activation, J. Ethnopharmacol. 292 (2022) 115196.
[18] K. Pohl, P. Moodley, A.D. Dhanda, Alcohol's impact on the gut and liver, Nutrients 13 (2021).
[19] P.T. Nunes, B.T. Kipp, N.L. Reitz, L.M. Savage, Aging with alcohol-related brain damage: critical brain circuits associated with cognitive dysfunction, Int. Rev. Neurobiol. 148 (2019) 101–168.
[20] Truque C. Porras, L.M. García Moreno, P.M. Gordo, X.G. Ordoñez, F. Cadaveira, M. Corral, Verbal memory and executive components of recall in adolescent binge drinkers, Front. Psychol. 14 (2023) 1239716.
[21] M. Liu, S. Guo, D. Huang, D. Hu, Y. Wu, W. Zhou, et al., Chronic alcohol exposure alters gene expression and neurodegeneration pathways in the brain of adult mice, J. Alzheim. Dis.: JAD 86 (2022) 315–331.
[22] K.E. Pleil, E.G. Lowery-Gionta, N.A. Crowley, C. Li, C.A. Marcinkiewcz, J.H. Rose, et al., Effects of chronic ethanol exposure on neuronal function in the prefrontal cortex and extended amygdala, Neuropharmacology 99 (2015) 735–749.
[23] Y. Qi, Q. Zhang, H. Zhu, Huang-Lian Jie-Du decoction: a review on phytochemical, pharmacological and pharmacokinetic investigations, Chinese medicine 14 (2019) 57.
[24] W.J. He, D.M. Cao, Y.B. Chen, J.J. Shi, T. Hu, Z.T. Zhang, et al., Explore of the beneficial effects of Huang-Lian-Jie-Du Decoction on diabetic encephalopathy in db/db mice by UPLC-Q-Orbitrap HRMS/MS based untargeted metabolomics analysis, J. Pharmaceut. Biomed. Anal. 192 (2021) 113652.
[25] J.Y. Zheng, X.X. Li, W.Y. Lin, S. Su, H.C. Wu, R.D. Hu, et al., Huang-Lian-Jie-Du decoction alleviates depressive-like behaviors in dextran sulfate sodium-induced colitis mice via Trem2/Dap12 pathway, J. Ethnopharmacol. 315 (2023) 116658.
[26] L.C. Walker, Aβ plaques, Free neuropathology 1 (2020).
[27] G. Pagni, C. Tagliarini, M.G. Carbone, B.P. Imbimbo, D. Marazziti, N. Pomara, Different sides of depression in the elderly: an in-depth view on the role of Aβ peptides, Curr. Med. Chem. 29 (2022) 5731–5757.
[28] Y. Liu, T. Du, W. Zhang, W. Lu, Z. Peng, S. Huang, et al., Modified huang-lian-jie-du decoction ameliorates Aβ synaptotoxicity in a murine model of Alzheimer's disease, Oxid. Med. Cell. Longev. 2019 (2019) 8340192.
[29] Y. Zheng, X.R. Cheng, W.X. Zhou, Y.X. Zhang, Gene expression patterns of hippocampus and cerebral cortex of senescence-accelerated mouse treated with Huang-Lian-Jie-Du decoction, Neurosci. Lett. 439 (2008) 119–124.
[30] A.A. Coley, W.J. Gao, PSD95: a synaptic protein implicated in schizophrenia or autism? Progress in neuro-psychopharmacology & biological psychiatry 82 (2018) 187–194.
[31] M.A. Cousin, Synaptophysin-dependent synaptobrevin-2 trafficking at the presynapse-Mechanism and function, J. Neurochem. 159 (2021) 78–89.
[32] C. Dorard, G. Vucak, M. Baccarini, Deciphering the RAS/ERK pathway in vivo, Biochem. Soc. Trans. 45 (2017) 27–36.
[33] R. García-Gómez, X.R. Bustelo, P. Crespo, Protein-protein interactions: emerging oncotargets in the RAS-ERK pathway, Trends in cancer 4 (2018) 616–633.
[34] A. Martin-Vega, M.H. Cobb, Navigating the ERK1/2 MAPK cascade, Biomolecules 13 (2023).
[35] S.T. Eblen, Extracellular-regulated kinases: signaling from Ras to ERK substrates to control biological outcomes, Adv. Cancer Res. 138 (2018) 99–142.
[36] C. Schanbacher, M. Bieber, Y. Reinders, D. Cherpokova, C. Teichert, B. Nieswandt, et al., ERK1/2 activity is critical for the outcome of ischemic stroke, Int. J. Mol. Sci. 23 (2022).
[37] Y. Zheng, L. Zeng, X. Dong, Q. Du, Y. Gao, Periostin aggravates the early phase of traumatic brain injury via the MAPK/ERK pathway, Neurol. Res. 44 (2022) 560–569.
[38] Z. Tang, W. Wang, Z. Liu, X. Sun, Z. Liao, F. Chen, et al., Blocking ERK signaling pathway lowers MMP-9 expression to alleviate brain edema after traumatic brain injury in rats], Nan fang yi ke da xue xue bao = Journal of Southern Medical University 40 (2020) 1018–1022.
[39] J. Zhong, RAS and downstream RAF-MEK and PI3K-AKT signaling in neuronal development, function and dysfunction, Biol. Chem. 397 (2016) 215–222.
[40] D. Feng, B. Wang, Y. Ma, W. Shi, K. Tao, W. Zeng, et al., The ras/raf/erk pathway mediates the subarachnoid hemorrhage-induced apoptosis of hippocampal neurons through phosphorylation of p53, Mol. Neurobiol. 53 (2016) 5737–5748.
[41] M. Bi, A. Gladbach, J. van Eersel, A. Ittner, M. Przybyla, A. van Hummel, et al., Tau exacerbates excitotoxic brain damage in an animal model of stroke, Nat. Commun. 8 (2017) 473.
[42] M.M. Gravandi, S. Abdian, M. Tahvilian, A. Iranpanah, S.Z. Moradi, S. Fakhri, et al., Therapeutic targeting of Ras/Raf/MAPK pathway by natural products: a systematic and mechanistic approach for neurodegeneration, Phytomedicine : international journal of phytotherapy and phytopharmacology 115 (2023) 154821.